

---

EARTH SCIENCES,  
GLACIOLOGY AND  
GLOBAL CHANGE

---



## **GPS derived Velocity Field and Strain Rates of Schirmacher Glacier, East Antarctica**

**P. S. Sunil<sup>1</sup>, C. D. Reddy<sup>1</sup>, Ajay Dhar<sup>1</sup>, M. Ponraj<sup>1</sup>,  
C Sevaraj<sup>1</sup> and D Jayapaul<sup>2</sup>**

<sup>1</sup> Indian Institute of Geomagnetism, New Panvel, Navi Mumbai - 410218.

<sup>2</sup> Geological Survey of India, Antarctica Division, Faridabad

### **ABSTRACT**

Monitoring of ice sheet velocity is one of the key issues to glacier dynamics understanding. Although the surface displacements of glaciers can be monitored Global Positioning System (GPS), this process is difficult in Antarctica due to logistic operations. Two GPS campaigns were conducted during the austral summer of 2003 and 2004 in the vicinity of Schirmacher Oasis, central Dronning Maud Land (cDML), East Antarctica to understand the velocity and strain rates of Schirmacher Glacier. GPS data was collected at 21 sites and have been analyzed to estimate the site co-ordinates, baselines and velocities. All the GPS sites on the glacier have been constrained, with the base station MAIT and the nearby IGS stations VESL and SYOG. Horizontal velocities of the glacier sites lie between  $1.89 \pm 0.01$  and  $10.88 \pm 0.01$  m/yr to the north-north-east, with an average velocity of  $6.21 \pm 0.01$  m/yr. The principal strain-rates provide a quantitative measurement of extension rates, which range from  $0.11 \pm 0.01 \times 10^{-3}$  to  $1.48 \pm 0.85 \times 10^{-3}$  yr<sup>-1</sup> and shortening rates, which range from  $0.04 \pm 0.01 \times 10^{-3}$  to  $0.96 \pm 0.16 \times 10^{-3}$  yr<sup>-1</sup>. The velocity and strain rate distributions across the GPS network in the Schirmacher Glacier are spatially correlated with topography, subsurface undulations, fracture zones/crevasses and the partial blockage of the flow by nunataks and Schirmacher Oasis.

### **INTRODUCTION**

The polar sea ice, ice caps in the periphery of the Antarctic continent, and inland ice, ice shelf systems are cryospheric indicators of climate change that react particularly sensitively to variations of regional to global climate parameters. As the Polar Regions contribute significantly to global sea-level change, it is therefore crucial to determine the mass balances of the

Antarctica Ice sheets. . The space geodetic techniques have a major impact on the study of glacier movement by making accurate measurements of the glacier surface. The satellite based navigation and surveying technique Global Positioning System (GPS) has an important role to understand the ice sheet dynamics and the repeated GPS measurements at an interval of time helps to determine the ice velocity very precisely. This surface velocity fields can provide useful information on the dynamics of the glacier and changes in the movement of the Antarctic ice sheet caused by Global Warming.

Glaciers surface displacements can be monitored by various means: the traditional technique, most commonly used, consists of fixing reference points on the glacier surface, and measuring their position at different times of the year. With the use of differential GPS, very precise measurement can be made. However, this method is limited to a few points in the accessible part of the glaciers. In places like Antarctica, where logistics is a major constrain for the inhospitable terrain and frequent bad weather spells, these campaigns can be carried out using Helicopters. This kind of field campaign is costly and may be difficult on occasions for poor visibility, flying conditions and bad weather. Frequent blizzards and heavy snow drift may result in covering some of the reference points. Aerial or satellite imagery have been used for such displacement measurement. The main advantage in such studies is the spatial coverage, potentially the whole glacier. Satellite radar interferometry has been used for precise ice velocity measurement since 1993 (Goldstein, 1993), and this technique is adequate for measuring small displacements (up to a few tens of cm), on cloud covered areas. This method has proved to be adequate to follow glaciers displacements over a few days.

The coastal region of Antarctica is the most sensitive part of the Antarctic system and 90% of the discharge from Antarctic ice sheet is through small number of ice streams and outlet glaciers. Schirmacher Glacier is one such important outlet glacier in central Dronning Maud Land (cDML), playing a major role in the drainage of East Antarctica (Fig. 1). It is located between an area south of the Lazarev Sea and Nivlisen Ice Shelf (Sengupta, 1986; Hermichen, 1995; Horwath et al., 2006) and north of Potsdam Glacier and Wohlthat Massif (Scheinert, 2001; Anschutz and others 2007). The study region is bounded by longitudes  $11^{\circ}10'E$  and  $12^{\circ}10'E$ , and latitudes  $70^{\circ}40'S$  and  $71^{\circ}00'S$ . Mean annual air temperature is below  $-20^{\circ}C$  (Bormann and Fritzsche, 1995). In general terms, the Schirmacher Glacier flow is blocked by the Schirmacher Oasis (a low lying nunatak) located to the north.



In the 1980s, glaciologists from the then East Germany explored some classical ice caves in Schirmacher Glacier, created by water flow. They are outflow conduits draining internal glacier water. With the availability of this vast amount of different types of informations for the past two decades, it has become a valuable site for observing the changes in the movement of the Antarctic ice sheet caused by global warming. Here, we describe the velocity and strain-rate fields obtained during two GPS campaigns undertaken on Schirmacher Glacier during two austral seasons of 2003 and 2004.

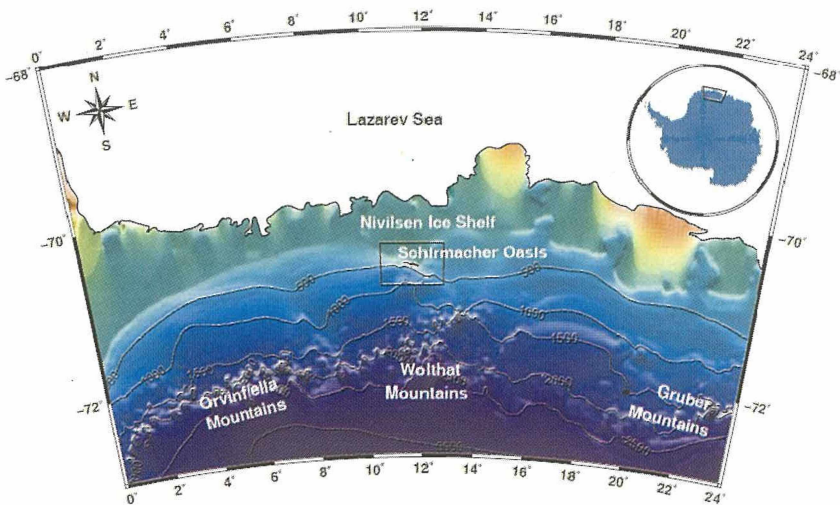


Fig. 1: Location map of central Dronning Maud Land, East Antarctica, showing the study area of Schirmacher Glacier (rectangle) superimposed on a shaded relief map of GTOPO30 digital elevation model with 500m elevation contour interval.

## SURVEY DESCRIPTION AND DATA PROCESSING

A network of 21 GPS sites with  $\sim 5$  km inter-station spacing was established covering an area of  $25 \times 50$  sq km (Fig. 3). The coordinates of these sites are given in Table 1. Dual frequency (L1/L2) geodetic Trimble 4000SSi receivers with choke ring antenna were used for the data collection. The GPS antennas were fixed on a 1.5-cm diameter threaded steel bolt fixed on a wooden block of  $1 \times 1 \times 2$  ft, embedded in ice up to a depth of 1.5 ft (Fig. 2a). The two campaigns were carried out during austral summers of 2003 and 2004. The data was collected at each site for about 48 hours with 30 seconds sampling interval. A permanent GPS is set up (shown with star

symbol in Fig. 3) on exposed bedrock at Maitri (Fig. 2b). Helicopters and snow vehicles were used for setting up the GPS receivers at field sites. The GPS receivers were powered by specially sealed 12V, 72AH charged batteries enclosed in non-conducting boxes. Due to logistic constraints during the second GPS campaign, the data could be collected at 15 sites only out of 21 sites installed during the first campaign in 2003. Data was downloaded to the Notebook PC and converted to Receiver Independent Exchange (RINEX) format at each site.

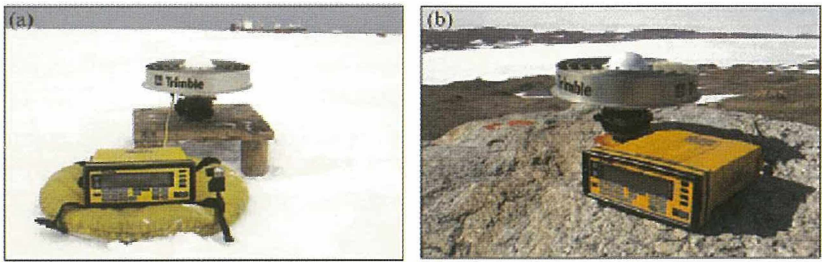


Fig. 2: (a) GPS antenna mounted on wooden platform on the glacier; (b) Set-up of the GPS base station on bedrock.

The data for both the campaigns were converted to daily files covering a UTC day to facilitate the processing related to nearby IGS (International GNSS Service) network sites VESL and SYOG (Fig. 3). All pseudo range and phase data were analyzed using GAMIT post-processing software developed by Massachusetts Institute of Technology and Scripps Institution of Oceanography (King and Bock, 2000). The data were analyzed for satellite state vectors, tropospheric zenith delay parameters and phase ambiguities using doubly differenced GPS phase measurements, to obtain estimates and an associated covariance matrix of station positions. Thus, for each session, a “loose solution” (Feigl et al., 1993) defined in the International Terrestrial Reference Frame 2000 (ITRF2000) (Altamimi et al., 2002) (by using precise orbits) has been obtained and then passed through a Kalman filter (Herring et al., 1990). In the second step, these loosely constrained solution files (h-files) were combined with the global solution files (IGS files) from the IGS daily processing routinely done at Scripps Institute of Oceanography (SIO) by using the GLOBK software (Herring, 2002). The ITRF2000 reference frame was imposed using this combined solution by minimizing the position and velocity deviation of IGS core stations SYOG and VESL with respect to the ITRF2000 for the estimation of consistent set of coordinates and velocities of each GPS site.

## GLACIER VELOCITY

The magnitudes of surface horizontal velocity estimated at each site of Schirmacher glacier are given in Table 1, and the velocity vectors are shown in Fig. 3 (for 15 sites out of 21 sites). The velocity vectors represent the spatial pattern of glacier movement across Schirmacher Glacier. The lowest velocity,  $1.89 \pm 0.01$  m/yr, and highest,  $10.88 \pm 0.01$  m/yr, were observed in the southeastern and northeastern parts of the study area, respectively, with an average velocity of  $6.21 \pm 0.01$  m/yr in the north-northeast direction, with error limits of 95% confidence. The resulting velocities show that the eastern part of the Schirmacher Oasis acts to funnel Schirmacher Glacier toward Nivlisen. The GPS sites 02, 04, 05, 06 and 07 (Fig. 3), which are located over the continental slope with maximum steepness, exhibit low velocities, i.e. the velocity distribution is such that it is lowest near the Schirmacher Oasis margin and highest near the eastern part where the blockage of Schirmacher Oasis is absent. Overall, the velocity distribution shows that velocities decrease away from Schirmacher Oasis and towards the continental ice.

**Table 1 : Geodetic co-ordinates of the GPS stations on Schirmacher Glacier with horizontal flow rates (in ITRF2000 at epoch 2004.0), azimuth and uncertainty. The dashed lines indicate absence of flow rates due to the inability to reoccupy stations during the second campaign.**

Glacier Points	Long. (East)	Lat. (South)	No. of Occupations	Horizontal Velocity ( $\text{m a}^{-1}$ )	Azimuth (Degree)	Uncertainty ( $\text{mm a}^{-1}$ )
GL01	11.441	-70.747	1	-----	-----	-----
GL02	11.463	-70.755	2	02.37	34.30	5.65
GL03	11.488	-70.768	1	-----	-----	-----
GL04	11.527	-70.781	2	04.33	34.14	6.63
GL05	11.571	-70.798	2	06.56	19.22	7.54
GL06	11.624	-70.797	2	06.97	19.05	7.77
GL07	11.671	-70.796	2	07.82	25.81	7.92
GL08	11.719	-70.800	1	-----	-----	-----
GL09	11.763	-70.806	2	08.81	34.28	8.26
GL10	11.808	-70.818	1	-----	-----	-----
GL11	11.789	-70.826	2	10.79	38.13	6.55
GL12	11.488	-70.867	2	04.85	28.08	6.41
GL13	11.453	-70.858	2	04.47	27.27	6.46
GL14	11.463	-70.855	1	-----	-----	-----
GL15	11.511	-70.888	1	-----	-----	-----
GL16	11.478	-70.926	2	02.84	26.78	8.38
GL17	11.637	-70.863	2	07.18	16.82	7.37
GL18	11.700	-70.885	2	10.88	30.56	9.48
GL19	11.746	-70.886	2	08.70	44.64	7.49
GL20	11.812	-70.946	2	04.69	41.07	8.40
GL21	11.859	-70.958	2	01.89	35.91	7.03



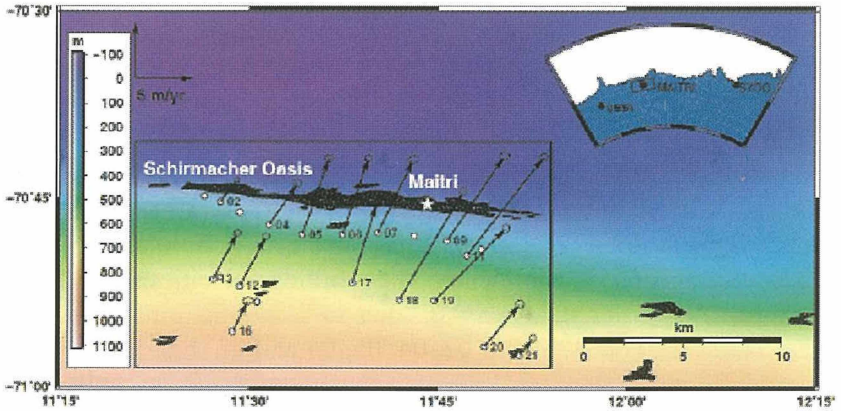


Fig. 3: Network of 21GPS sites in Schirmacher Glacier and horizontal velocity vectors (with 95% confidence ellipses) for the 15 GPS sites, superimposed on a shaded relief map of GTOPO30 topographic data. In the inset, the rectangle indicates the study region near Indian research station MAITRI and the IGS stations VESL and SYOG.

## STRAIN RATES

Since triangulation techniques provide large spatial variability of the strain-rate pattern and are more sensitive to single station velocities and inter-site distances (Serpelloni et al., 2005) we divided the Schirmacher Glacier network into 18 triangular sub-networks to study the strain-rate distribution. Using a standard least-squares procedure (Feigl et al., 1990) we computed the horizontal strain-rate tensor within each region. Further, we derived the rates of dilatation and shear strains in the direction of the principal strain axes. The triangular regions and estimated horizontal principal axes, dilatational and shear strains are shown in Figs. 4, 5 and 6 respectively. We computed the spatial distribution of the principal strain rate ( $\dot{\epsilon}$ ) and the principal axis azimuth ( $\delta$ ) for the Schirmacher Glacier sites over a period of one year. The compressional strain rate ( $\dot{\epsilon}_{\text{com}}$ ) ranges from  $0.04 \pm 0.01 \times 10^{-3}$  to  $0.96 \pm 0.16 \times 10^{-3} \text{ yr}^{-1}$  with high compressional strain rates of  $0.83 \pm 0.23 \times 10^{-3}$ ,  $0.72 \pm 0.43 \times 10^{-3}$  and  $0.96 \pm 0.16 \times 10^{-3} \text{ yr}^{-1}$  observed in the triangular regions A, C and M, respectively. The extensional strain rates ( $\dot{\epsilon}_{\text{ext}}$ ) are in the range  $0.11 \pm 0.01 \times 10^{-3} \text{ yr}^{-1}$  (triangle A of Fig. 5, close to the Schirmacher Oasis) to  $1.48 \pm 0.85 \times 10^{-3} \text{ yr}^{-1}$  (triangle J, located to the south-east of Schirmacher Oasis). The EW to NNE trending maximum extensional strains occur in the triangular regions H, J, K, Q and R, which are located in the eastern part of the glacier, where velocities are high.

Where as, minimum amount of compressional as well as extensional strain rates found in the triangular area F. This pattern is due to acceleration along divergent flow lines in the east of Schirmacher Glacier. The high dilatation and shear strain rate distributions well correlates with the blockage of the Schirmacher Oasis and Glacier flow towards northeast direction respectively.

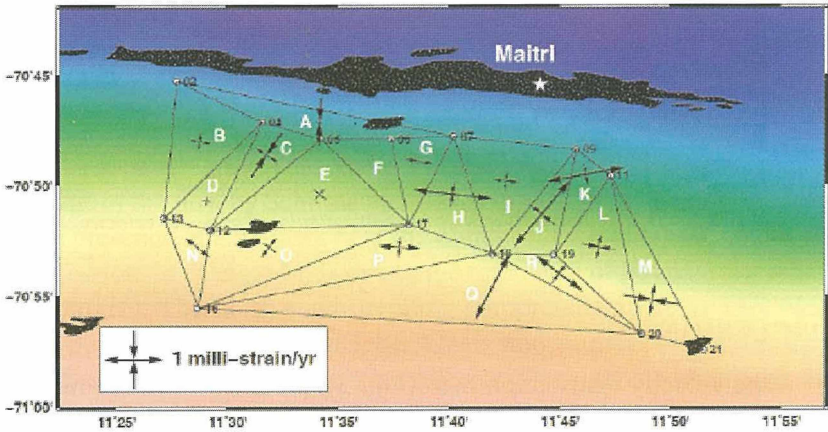


Fig. 4: Spatial distribution of the principal strain rates for triangular regions. The outward and inward arrows display extension and contraction respectively. Co-ordinates of the barycentres of these triangles are given in Table 2

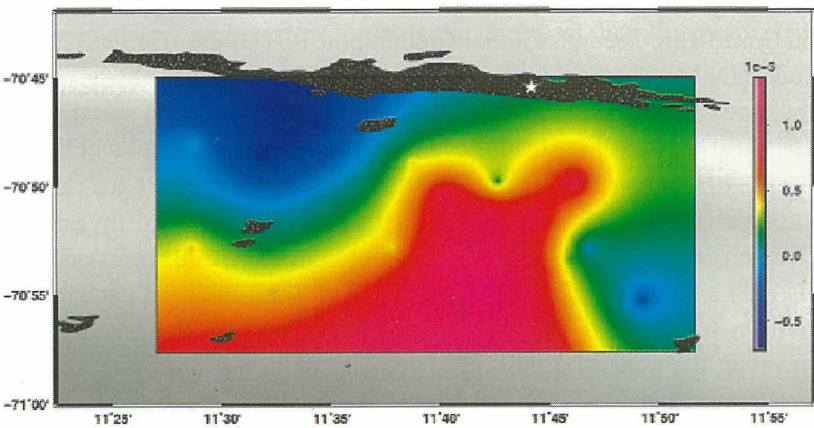
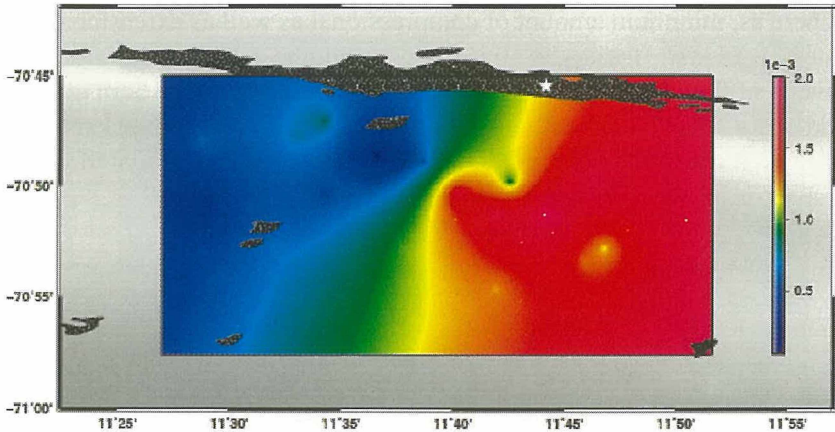


Fig. 5: Distribution of dilatational strain rate calculated from the velocity field shown in Figure 3



*Fig. 6: Distribution of shear strain rate calculated from the velocity field shown in Figure 3*

## DISCUSSION

The velocity distribution map (Fig. 3), prepared from the measured station velocities, shows the trend of the glacier flow towards the NNE direction into the Nivlisen Ice Shelf. The map shows a less velocity in the southwestern part of the area and gradual increase up to a maximum of  $\sim 11$  m/yr in the ice shelf area towards the northeastern part of the glacier. The high velocity region shown on the map consists of GPS sites 09, 11, 18 and 19. Though the gentle slope is observed in this region during the field survey and from 30 arc-seconds Global Topographic (GTOPO30) Digital Elevation Model (DEM), the maximum velocity seen in this part is due to the minimum blockage of Schirmacher Oasis. At GPS sites 02, 04, 05, 06 and 07, despite their location over the steep elevation gradient region, the velocity is low because of the resistance to the flow due to the Schirmacher Oasis blockage. The results from this study agree with previous geodetic investigations (Dietrich et al., 1999; Metzger et al., 2000; Scheinert, 2001) carried out near this area and show that the major outlet of Schirmacher Glacier towards Nivlisen Ice Shelf is through the eastern end of the Schirmacher Oasis. However, the general trend of the velocity pattern shows that, away from the Schirmacher Oasis towards the continental ice, the velocity decreases due to the very gentle slope in the continental ice surface and the presence of nunataks. A Ground Penetrating Radar (GPR) study conducted south of our study area, in Potsdam Glacier (Fig. 1), indicates evidence of subsurface



undulations with an ablation area in the southeastern part of the Schirmacher Glacier (Anschutz et al., 2007), also contributes to the reduction of velocity from north to south in the continental ice. Measured surface velocities for the Schirmacher Glacier (with maximum velocity  $\sim 11$  m/yr) are much lower than the velocities of Shirase Glacier (2700 m/yr) which lies in a narrow trough less than 10 km wide (Pattyn and Derauw, 2002; Pattyn and Naruse, 2003). However, they are closer to those of the Lambert Glacier (10 - 25 m/yr) (Manson et al., 2000) and Potsdam Glacier (20 - 30 m/yr at higher elevations and 70 - 80 m/yr at lower elevations) (Dietrich et al., 1999; Anschutz et al., 2007) which also flow into ice shelves and which have similar surface trends.

As seen in Figure 4, the compressional strain rate in triangle A indicates blockage of the flow by Schirmacher Oasis. In triangle C, the flow is affected by the presence of a nunatak near the points GL05 and GL06. The highest compression, in triangle M, is due to the resistance of Pevikhornet nunatak (near GL21). The north-south trending compressional strain axes clearly bring out the role of Schirmacher Oasis and nunataks in defining the compressive regime in Schirmacher Glacier. The highest extensional strain rates occur in triangle regions H, J, K, Q and R, which show the occurrence and contribution of steep and shallow criss-cross fracture zones and crevasses in the high velocity region. The EW to NNE trend of the extensional strain rates also follows the divergence of the Schirmacher Glacier towards the Nivlisen Ice Shelf. These features are also seen in the dilatational and shear strain distributions and support the blockage of Schirmacher in the northern part of the glacier and its flow towards the northeast direction respectively.

## **CONCLUSIONS**

To study the velocity and strain distribution of the Schirmacher Glacier in East Antarctica, GPS data has been collected for two campaigns during austral summer of 2003 and 2004 and analyzed using GAMIT/ GLOBK software. The glacier velocity results show that the magnitude of the horizontal velocity is in the range of 1.89 to 10.88 m/yr with an average of 6.21 m/yr, in the NNE direction. The distribution of velocity can be spatially correlated with topography, subsurface undulations, fractures/crevasses (coinciding with high velocities), and the influence of the blockage of Schirmacher Oasis. The surface strain analysis indicates that the direction of principal axes, dilatation and shear strain rates supports the region of extensional in coincides with the surface gradient and crevasses and blockage of Schirmacher Oasis. The general trend to low (compared to other glaciers) velocities ( $\sim 11$  m/yr)

is primarily attributed to the fact that Schirmacher Glacier is located in a region of exposed nunataks which extend along the ice shelf grounding line. The InSAR results with good vertical resolution can supplement the GPS results with good horizontal resolution.

## ACKNOWLEDGEMENTS

The study was supported by Department of Science & Technology, Govt. of India. This study was carried out under a collaborative program of Indian Institute of Geomagnetism (IIG) and Geological Survey of India (GSI), Antarctica Division. We sincerely thank the Directors of the Indian Institute of Geomagnetism and Geological Survey of India (Antarctica Division) for their support to carry out this study in Antarctica. The study was suggested by Dr. R Ravindra, Director, National centre for Antarctic & Ocean Research, and his help in making the specially designed monuments for installing GPS Antennas is sincerely acknowledged. We are grateful to Mr. M. Doiphode (IIG), Mr. Kuldip Kachroo and Mr. Rajesh Asthana (GSI) and Mr. Shailendra Saini (BU) for extending their support in deployment of GPS receivers in most hostile conditions. We thank Prof. Bob King for making GLOBK/GAMIT GPS data analysis software available and P. Wessel and W.H.F. Smith for their GM Tools.

## REFERENCES

1. Altamimi, Z., P. Sillard and C. Boucher. 2002. ITRF2000: A new release of the International Terrestrial Reference Frame for earth science applications. *J. Geophys. Res.*, 107(B10), 2214, doi:10.1029/2001JB000561.
2. Anschutz, H., O. Eisen, H. Oerter, D. Steinhage and M. Scheinert. 2007. Investigating small-scale variations of the recent accumulation rate in coastal Dronning Maud Land, East Antarctica. *Ann. Glaciol.*, 46, 14-21.
3. Bormann, P. and D. Fritzsche, eds. 1995. *The Schirmacher Oasis, Queen Maud Land, East Antarctica, and its surroundings*. Gotha, Justus Perthes Verlag.
4. Dietrich, R., R. Metzger, E. Korth and J. Perlt. 1999. Combined use of field observations and SAR interferometry to study ice dynamics and mass balance in Dronning Maud Land, Antarctica. *Polar Research*, 18(2), 291-298.
5. Feigl, K.L., R.W. King and T.H. Jordan. 1990. Geodetic measurement of tectonic deformation in the Santa Maria Fold and Thrust Belt, California. *J. Geophys. Res.*, 90, 2679-2699.
6. Feigl, K.L., R.W. King, T.A. Herring and M. Rothacher. 1993. Space geodetic measurement of crustal deformation in central and southern California, 1984-1992. *J. Geophys. Res.*, 98, 21677-21712.



7. Goldstein, R. M., H. Engelhardt, B. Kamb and R.M. Frolich. 1993. Satellite radar interferometry for monitoring ice-sheet motion: application to an Antarctic ice stream. *Science*, 262, 1525-1530.
8. Herring, T.A. 2002. GLOBK: Global Kalman Filter VLBI and GPS Analysis Programme Version 10.0, Massachusetts Institute of Technology, Cambridge. Herring, T.A., J.L. Davis and I.I. Shapiro. 1990. Geodesy by radio interferometry: The application of Kalman filtering to the analysis of very long baseline interferometry data. *J. Geophys. Res.*, 95, 12561-12581.
9. Hermichen, W. (1995) The continental ice cover in the surroundings of the Schirmacher Oasis. In: Bormann, P. and Fritzsche, D. (Eds), The Schirmacher Oasis, Queen Maud Land, East Antarctica, and its surroundings, pp. 221-242.
10. Horwath, M., R. Dietrich, M. Baessler, U. Nixdorf, D. Steinhage, D. Fritzsche, V. Damm and G. Reitmayr. 2006. Nivlisen, an Antarctic Ice Shelf in Dronning Maud Land: Geodetic-glaciological results from combined analysis of ice thickness, ice surface height and ice flow observations. *J. Glaciol.*, 52(176), 17-30.
11. King, R.W. and Y. Bock. 2000. Documentation for the GAMIT analysis software, release 10.0, Massachusetts Institute of Technology, Cambridge, U.K.
12. Manson, R., R. Coleman, P. Morgan and M. King. 2000. Ice velocities of the Lambert Glacier from static GPS observations. *Earth Planet Space*, 53, 1031-1036.
13. Metzig, R., R. Dietrich, W. Korth, J. Perlt, R. Hartmann and W. Winzer. 2000. Horizontal Ice velocity estimation and grounding zone deflection in the surrounding of Schirmacheroase, Antarctica, using SAR interferometry. *Polarforschung*, 67(1/2), 7-14.
14. Pattyn, F. and R. Naruse. 2003. The nature of complex ice flow in Shirase Glacier catchment, East Antarctica. *J. Glaciol.*, 49(166), 429-436.
15. Scheinert, M. 2001. Geodynamic investigations in Dronning Maud Land/Antarctica. *Journées Luxembourgeoises de Géodynamique*, 89, 12-14.
16. Sengupta, S. (1986) Geology of Schirmacher Range (Dakshin Gangotri), East Antarctica. Third Indian Expedition to Antarctica, Scientific report, pp. 187-217.
17. Serpelloni, E., M. Anzidei, P. Baldi, G. Casula and A. Galvani. 2005. Crustal Velocity and strain-rate fields in Italy and surrounding regions: new results from the analysis of permanent and non-permanent GPS networks. *Geophys. J. Int.*, 161, 861-880.